

## Selective Determination of Tetracycline in Broiler Chicken Meat by Molecularly Imprinted Polymer

Shendi Suryana\*, Aji Najihudin, Salma Elivania, and Meillia Suherman

Faculty of Mathematics and Natural Sciences, Department of Pharmacy, Universitas Garut, Garut - Indonesia

### Abstract

Tetracycline (TC) residues in poultry meat products can create antibiotic resistance in humans who consume them. Hence, sensitive analytical procedures to evaluate the quantities of tetracycline residues are required to assess the safety of these products for consumption. The study aimed to develop a sorbent using molecular imprinting technology to analyze tetracycline in chicken broiler meat products. The study used several tests and computational techniques to increase the effectiveness of screening for the best MIP systems. According to the bond energy-based computational analysis, methacrylate acid (MAA) was the best functional monomer at a TC-to-MAA molar ratio of 1:6. The mixture of methanol and chloroform yielded the greatest  $K_a$ . The Job plot showed that a TC-to-MAA-molar ratio of 1:6 was best for synthesizing imprinted polymer in the mixture of methanol and chloroform. We generated MIPs using two alternative production methods: bulk (MIP1) and precipitation (MIP2). Adsorption capacity results revealed that MIP1 matches well with the Langmuir model, whereas MIP2 fits better with the Freundlich. MIP1 application produced recovery rates of  $82,74 \pm 4,1\%$  and MIP2 results of  $92,14 \pm 3,2\%$  for TC in spike-chicken meat. The outcomes of the selectivity test also demonstrated that MIP2 is superior to MIP1 and can recover TC from spiked chicken meat while coexisting with another antibiotic drug. The study's findings indicate that MIP2 helps determine TC in spike chicken meat.

**Keywords:** Broiler chicken meat, molecularly imprinting polymer, tetracycline.

## Polimer Tercetak Molekul Untuk Ekstraksi Selektif Tetrasiklin Dalam Daging Ayam Ras

### Abstrak

Polimer tercetak molekul (PTM) disintesis untuk ekstraksi secara selektif residu tetrasiklin (TC) dalam daging ayam ras. Penelitian ini menggunakan berbagai uji dan teknik komputasi untuk meningkatkan efektivitas seleksi sistem PTM terbaik. Menurut energi ikatan berbasis analisis komputasi, asam metakrilat (MAA) adalah monomer fungsional terbaik pada rasio molar TC-MAA sebesar 1:6. Campuran metanol dan kloroform menghasilkan  $K_a$  terbesar. Analisis Job Plots menunjukkan bahwa rasio molar TC-MAA sebesar 1:6 adalah yang terbaik untuk mensintesis polimer bercetakan dalam campuran metanol dan kloroform. Polimer disintesis menggunakan dua metode: ruah (PTM1) dan pengendapan (PTM2). Hasil kapasitas adsorpsi mengungkapkan bahwa PTM1 cocok dengan model Langmuir, sedangkan PTM2 lebih cocok dengan Freundlich. Aplikasi PTM1 menghasilkan perolehan kembali sebesar  $82,74 \pm 4,1\%$  sedangkan PTM2 sebesar  $92,14 \pm 3,2\%$  untuk ekstraksi TC dalam daging ayam ras. Hasil uji selektivitas juga menunjukkan bahwa PTM2 lebih unggul daripada PTM1 dalam ekstraksi TC dari daging ayam ras yang di-spike dengan TC bersama dengan obat antibiotik lainnya. Hasil penelitian menunjukkan bahwa PTM2 efektif dalam menentukan TC dalam daging ayam ras.

**Kata Kunci:** Daging ayam broiler, polimer tercetak molekul, tetrasiklin.

### Article History:

Submitted 06 November 2024

Revised 27 January 2025

Accepted 05 February 2025

Published 17 May 2025

\*Corresponding author:

[shendi@uniga.ac.id](mailto:shendi@uniga.ac.id)

### Citation:

Suryana, S.; Najihudin, A.; Elivania, S.; Suherman, M. Selective Determination of Tetracycline in Broiler Chicken Meat by Molecularly Imprinted Polymer. Indonesian Journal of Pharmaceutical Science and Technology. 2025: Vol. 12 Suppl. 2: 130-139.

## 1. Introduction

Tetracycline (TC) is one of the most widely used antibiotics in animal husbandry. It is a feed supplement that promotes animal growth and prevents and treats disease.<sup>1</sup> Its broad-spectrum antibacterial action and low cost are among its benefits.<sup>2</sup> However, TC overuse can leave residues in food that impair liver and kidney function and have teratogenic, carcinogenic, and mutagenic effects on consumers.<sup>3</sup> More stringent regulations about food tetracycline residues have been implemented to ensure food safety.

Concerns about the effects of this antibiotic's presence in food samples on public health have surfaced in recent years.<sup>4</sup> Relatively high TC residue levels in food can spread drug-resistant germs from food to people and cause allergic reactions in certain hypersensitive people.<sup>5</sup> Exposure to low residue levels has both long-term and immediate consequences. Consequently, much work has gone into creating and confirming analytical techniques that can measure TC in food samples.<sup>6</sup>

Food analysis has included several sample pretreatment techniques, including liquid-liquid extraction (LLE),<sup>7</sup> extractions in the solid phase (SPE),<sup>8</sup> solid-phase microextraction (SPME),<sup>9</sup> and supercritical fluid extraction (SFE).<sup>10</sup> However, these techniques still have low adsorption capacity and selectivity issues, lengthy procedures, and high organic solvent usage.<sup>11</sup> So, novel approaches for selective adsorption, enrichment, and separation of tetracycline from complex dietary matrices must be developed.

The ability of molecularly imprinted polymers (MIPs) to recognize certain compounds in complicated mixtures has garnered significant attention from researchers as a potential purifying sorbent.<sup>12</sup> Furthermore, MIPs have high-temperature stability, high-pressure stability, and extreme pH stability in a range of challenging settings, and they can be recycled multiple times.<sup>13</sup> MIPs are,

therefore, prospective sorbents in the residue analysis field.<sup>14</sup>

Tetracycline analysis will be conducted using a novel solid-phase extraction technology developed in this study. Tetracycline will be incorporated into the polymer during construction, as a template for studying chicken boiler meat.

## 2. Materials and Methods

### 2.1. Tools

Hyperchem 8.0.10 was used for molecular geometry optimization to anticipate binding sites and calculate binding energy ( $\Delta E$ ). The sorbent's surface area was determined using the Brunauer, Emmett, and Teller (BET) Surface Area Quantachrome (Nova 4200E, Boynton Beach, USA). The morphological examination was conducted Using scanning electron microscopy with energy dispersive spectroscopy (SEM/EDS; JEOL JSM-6360 LA Japan), and FTIR (Fourier transform infrared spectroscopy). Using an ultraviolet-visible (UV-Vis) spectrophotometer (Shimadzu, Japan), the UV absorbance was measured to determine the association constant ( $K_a$ ) and create the Job plot. An Ohaus Pioneer digital balance, a centrifuge (Hettich, Germany), and a 50-watt 40 kHz ultrasonicator (NEY 19H, Houston, Texas, USA) were employed.

### 2.2. Materials

The following materials were used in this study: distilled water, methylacrylic acid (MMA) product number 155721 (Sigma Aldrich), chloroform product number 107024 (Merck), benzoyl peroxide (BPO) product number 801641 (Merck), ethylene glycol dimethacrylate (EGDMA) product number 335681 (Sigma Aldrich), methanol product number 113351 (Merck), potassium bromide product number 104904 (Merck), oxytetracycline (OTC) product number 500105, tetracycline (TC) product number 87128,

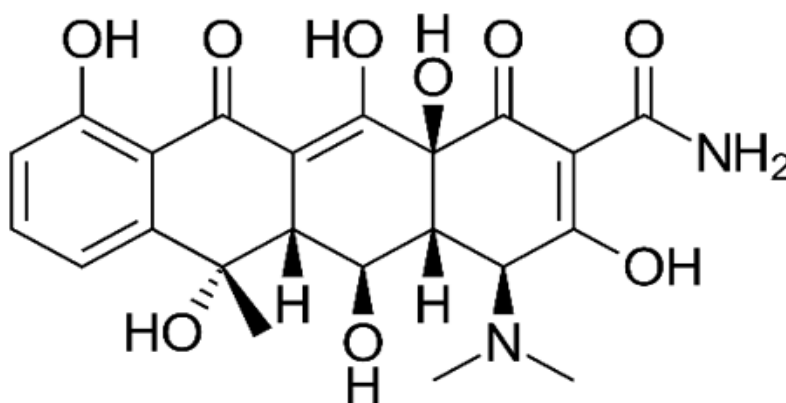


Figure 1. Chemical Structure of Tetracycline

and chlortetracycline (CTC) product number 500105 (Sigma Aldrich). The grade quality of all the materials was excellent, and the analytical grade was excellent.

An explanation of TC's HPLC requirements has been given. The process was carried out using Waters Alliance e2695 HPLC equipment with a UV detector, US. A Zorbax Eclipse XDB-Column C18 (4.6 × 150 mm, 5 µm) from Agilent Technologies (Santa Clara, CA, USA) was used for isocratic separation. A mobile phase consisting of 0.05 M oxalic acid buffer (pH 1.7)/acetonitrile/methanol (70:20:10, v/v/v) at a flow rate of 1 ml/min was used to produce the best separation. TC was detected at a wavelength of 357 nm. Calibration standards were examined in each run, and a 20 µl injection volume was used.

## 2.3. Methods

### 2.3.1. Functional monomer selection using computation

To determine the functional monomer computationally, three-dimensional (3D) structures of monomers and molecular templates were created using the Hyperchem 8.0.10 program.<sup>15</sup> Structure optimization used the semi-empirical restricted Hartree-Fock (RHF) approach. The PM3 technique optimized the complex between the template and the functional monomer using the self-consistent field (SCF) and RHF. The convergence value was 0.01 kcal when optimizing molecule shape using the "Polak-Ribière" gradient conjugate technique.

$$\Delta E = (E_{\text{complex}}) - (E_{\text{TC}} + E_{\text{functional monomer}}) \quad (1)$$

### 2.3.2. Ka calculation for the template's functional monomer complex

Before polymer production, the computational outcomes of the monomer-template interaction were assessed. The evaluation method used UV-vis spectrophotometry.<sup>16</sup> In a methanol-chloroform combination (1:1), functional monomers (FM) were added progressively up to 0.020 mol/l of tetracycline solution to obtain excess functional monomers. Ka was computed using the absorbance values that were obtained and delta absorbance curves for various monomer concentrations with the following equations:

$$\frac{1}{\Delta Y} = \frac{1}{Y_{\Delta \text{OTC-FM}}} Ka[FM] + \frac{1}{Y_{\Delta \text{OTC-FM}}} \quad (2)$$

Ka is the association constant, and ΔY is the absorbance; = OTC-FM complex absorbance - OTC absorbance.

### 2.3.3. Analysis of Job's Plot Stoichiometry

To undertake stoichiometric analysis, a molar ratio plot was created by systematically altering the molar ratio

of TC-MAA in a methanol-chloroform combination. We utilized 0.01 M and 0.002 M for MAA and TC, respectively. In total, there were three milliliters of TC-MAA. An absorbance plot was produced by dividing the absorbance by the molar concentration of TC.<sup>17</sup>

### 2.3.4. MIP and non-imprinted polymer (NIP) synthesis

#### *MIP Synthesis Using Bulk Polymerization*

Five milliliters of methanol-chloroform (1:1) and 0.2663 grams of tetracycline (TC) were mixed in a covered container. The TC was then sonicated for five minutes to dissolve completely in the liquid. 340 µL of MAA was added, and the mixture was then sonicated for 20 minutes. 3.77 mL of ethylene glycol dimethacrylate (EGDMA) was added as a crosslinker, and the mixture was sonicated for five minutes. The liquid should be sonicated for 20 minutes (until dissolved) after adding 125 mg of benzoyl phosphate (BPO) as an initiator. The vial was wrapped in parafilm and roasted for one hour at 70°C. After that, the vial was stored for eighteen hours at 70°C in a water bath. The substance was subsequently extracted using a Soxhlet extractor.<sup>18</sup>

#### *MIP Synthesis using Precipitation Polymerization*

Tetracycline (template, 0.2663 g) was dissolved by sonication in a closed glass bottle of 50 mL of methanol-chloroform (1:1). After adding 300 milliliters of methanol-chloroform and 340 µl of MAA, the mixture was sonicated for 20 minutes. 3.77 milliliters of ethylene glycol dimethacrylate (EGDMA) crosslinker were added, and the mixture was sonicated for five minutes. The chemical was completely dissolved when 250 mg of azobis-2-methylpropionitrile (AIBN) was sonicated for 20 minutes as an initiator. The bottle was wrapped in clingfilm and roasted at 70°C for one hour. 18 hours were spent with the vial in a water bath shaker set to 70°C.<sup>19</sup>

### 2.3.5. Physical characterization

FTIR spectroscopy was employed to characterize the functional groups in MIP and NIP, FTIR spectroscopy was employed.<sup>20</sup> The mixture was mashed until smooth and shaped into pellets after adding MIP and NIP in amounts up to 2 mg and potassium bromide (KBr) in amounts up to 200 mg. MIP or NIP's infrared spectrum measurement range was 4000–400 cm<sup>-1</sup>. Both before and after extraction, the MIP/NIP sorbents' functional groupings were identified. The composition of the elements and surface morphology of the polymer were investigated using SEM-EDS. MIP or NIP was added to the SEM after being inserted in silicon.<sup>21</sup> The MIP and NIP particle size distribution data were produced using PSA. The specific surface areas of MIP and NIP

were computed using BET. Nitrogen gas is allowed to flow across a particular surface area to calculate the amount of gas adsorbed on the surface using the BET technique. This procedure involved degassing 0.5 g of beads in a nitrogen gas stream for an hour at 150°C while in a sample container. Desorption happened at ambient temperature, however nitrogen gas adsorption was done at 210°C. The instrumental measurements made during the desorption phase were used to determine the beads' specific surface area.

#### 2.3.6. Evaluation of MIP and NIP adsorption capacity

MIP's adsorption capability was assessed using TC solution at 0, 0.25, 0.5, 0.75, 1, 1.5, 2, and 2.5 mg/l. A vial containing 20 mg of MIP sorbent was filled with 1.5 ml of TC solution, and the vial was left to remain at room temperature for a whole day. The HPLC was then used to determine the area under the curve. NIP sorbent was also used in the experiment. MIP adsorption capacity data were evaluated using adsorption curves from Freundlich and Langmuir isotherms.

#### 2.3.7. Use of MIP to extract TC from spiked chicken boiler meat

##### *MI-SPE condition optimization*

Solid-phase extraction cartridges made of empty plastic were used in this study. The dry polymer (200 mg) was put into the cartridges with frits on either end. They were called MISPE and NISPE. During the SPE process, the 12-port Phenomenex SPE vacuum manifold was used. After adding 1 ml of chloroform and holding it for five minutes, the mixture was vacuum-released to finish the conditioning process. The loading stage involved adding 1 milliliter of a 2 mg/L TC standard solution to chloroform, which was then left for 10, 15, 20, 25, 30, 35, and 50 minutes. It was then injected into the HPLC apparatus after being vacuum-released. MI-SPE or NI-SPE was cleaned with one milliliter of acetonitrile, left to sit for five minutes, released under vacuum, and injected into the HPLC apparatus. The last step, the elution stage, involved injecting 1 ml of a 9:1 methanol: acetic acid mixture into an HPLC system, letting it sit for 10 minutes, and then releasing it under vacuum.

##### *Application of MI-SPE and NI-SPE to spiked chicken boiler meat*

Using a household blender, 10 g of chicken meat was homogenized. Subsequently, the specimens were put into a 50 mL polypropylene centrifuge tube that held 20 mL of 25 mM ammonium acetate (pH 9) and underwent a 2-minute vortex mixing process. The supernatant was poured into a fresh centrifuge tube after the sample

was centrifuged for 10 minutes at 10 °C at 5000 rpm/min. To create spiked samples, a tetracycline standard solution was added to the previously mentioned solution until the final tetracycline concentration was 2 mg/L.

A standard TC solution was applied to spiked chicken meat. 200 mg of MIP and NIP were each contained in 3 mL SPE cartridges. SPE optimization was done with various solvents to obtain the best conditions for the conditioning, washing, and eluting phases. The optimal environment was determined using the highest recovery percentage discovered by HPLC analysis.

##### *Evaluation of MI-SPE selectivity for TC in spiked chicken boiler meat*

The treated chicken boiler meat was mixed with 2 mg/L of oxytetracycline (OTC), tetracycline (TC), and chlortetracycline (CTC). The sample was then spiked and passed through an NI-SPE or MI-SPE sorbent afterward. The elution outcomes were analyzed using HPLC. The recovery percentages were calculated for every MIP and NIP sorbent, molecule.

### 3. Result

#### 3.1. Functional monomer selection using computation

Ten functional monomers frequently employed to create imprinted polymers are shown in Table 1 along with their interactions with the template (TC) using  $\Delta E$ .  $\Delta E$  demonstrates the creation of complex stability. A low  $\Delta E$  number will result in persistent complex interactions and selective MIP synthesis because of its negative value. Three complexes had the lowest energy interaction energy: methacrylic acid (MAA), itaconic acid (ITA), and methyl methacrylic acid (MMA). Their respective  $\Delta E$  values were -29,3964173, -28.8437235, and -27.3776493 kcal/mol. Each molecule's low  $\Delta E$  suggested that the final MIP will be highly selective. The amount of monomer interacting with the template to determine reaction stoichiometry is computed to derive initial estimates for the MAA: TC molar ratio utilized during the synthesis process. Figure 2 depicts the intricate relationships between TC and monomers, particularly regarding MAA monomers.

#### 3.2. Calculating the $K_a$ for the functional monomer complex of the template

The  $K_a$  for template-functional monomer complexes was ascertained by applying UV-Vis spectrophotometry.<sup>27</sup> We considered MAA, ITA, and MMA based on the computational results. The  $K_a$  is connected with the functional monomer's affinity for binding to the template. To determine the TC-MAA

**Table 1.** The  $\Delta E$  values of the template-functional monomer complex

Template-functional monomer complex	$\Delta E$ (Kcal/mol)	Composition
Methacrylic acid (MAA)	-29.3964173	1:6
Itaconic acid (ITA)	-28.8437235	1:6
Methyl Methacrylic acid (MMA)	-27.3776493	1:6
Acrylic Acid (AA)	-25.7253647	1:4
2-Hydroxyethyl methacrylate (HEMA)	-22.5283952	1:5
Acrylamide (AAM)	-21.6359243	1:6
4-Vinylpyridine (4-VP)	-20.3726962	1:5
2-Vinylpyridine (2-VP)	-19.2836453	1:6
Trifluoro-methacrylic acid (TFMAA)	-17.29332411	1:5

$K_a$ , we added progressively more functional monomer (0.05 mol/L) to the TC solution in four distinct solvents: acetonitrile, methanol, chloroform, and a mixture of methanol and chloroform (1:1). Delta absorbance was plotted and recorded. Computing  $K_a$  involves collecting absorption data and using “Benesi Hildebrand” data analysis to produce graphs based on the intersection.<sup>28</sup> The methanol-chloroform combination solvent has the highest  $K_a$  value for the TC–MAA complex (Table 2).

### 3.3. Stoichiometry analysis (Job plot)

Polymer synthesis process design may benefit from the analysis of complex molecular ratios. The TC–MAA complex was assessed before polymerization using the Job’s Plot technique.<sup>28</sup> A method frequently employed in several approaches such as UV-Vis spectrophotometry is utilized to calculate the stoichiometry of complex interaction. Variations in the spectra of the host molecule (TC) and the guest molecule (functional monomer) are observed using this technique. <sup>29</sup> Measured at a wavelength of 357 nm was the solvent absorbance of both component solutions in methanol-chloroform (1:1). The absorbance peaked at a 1:6 molar ratio between the template and functional monomer and increased with

increasing TC concentration. An increase in functional monomers results in a decrease in absorbance.<sup>30</sup>

### 3.4. MIP and NIP synthesis with bulk and precipitation polymerization method

The two-method synthesis aimed to determine the efficacy of each polymer generated. Each approach had benefits and drawbacks of its own. Bulk polymerization has the following benefits: the mixture’s compound is in a liquid state without the need for an additional solvent; the resulting MIP’s particle size is easy to control; it is inexpensive when compared to other methods; and it is simple to carry out. On the other hand, the obtained MIP needs to be ground; there aren’t many variations in particle shape; and binding sites may be destroyed during the MIP grinding and sieving process.<sup>31</sup> The polymers resulting from the bulk method are called MIP1 and NIP1. The benefits of precipitation include the following: The process is simple and takes less time, the polymer chains grow separately into microspheres, the MIP beads have a regular shape and a good yield, and the only disadvantage is that precipitation happens when the polymer chains are big enough not to require porogen agents in the reaction mixture.<sup>32</sup> The polymers resulting from the precipitation

**Table 2.** Association constant value of TC with three monomer functionals in various solvent

No	Monomer	Solvent	$K_a$ (M-1)
1.	Methacrylic Acid (MAA)	Methanol	261.95
		Chloroform	1398.82
		Acetonitrile	748.93
		methanol-chloroform	2749.32
2.	Itaconic Acid (ITA)	Methanol	106.31
		Chloroform	1252.43
		Acetonitrile	839.92
		methanol-chloroform	2153.34
3.	Methyl Methacrylate (MMA)	Methanol	77.384
		Chloroform	1023.9
		Acetonitrile	293.48
		methanol-chloroform	1511.05



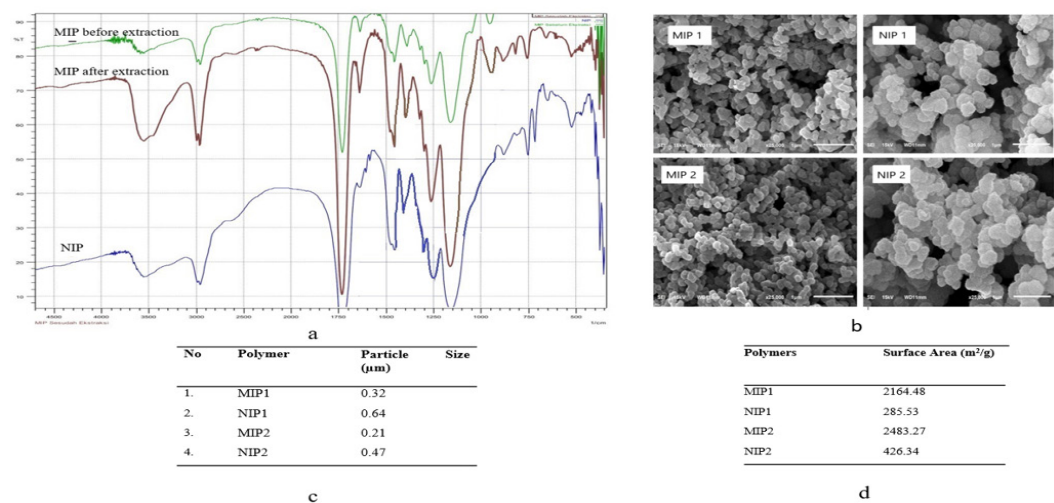


**Figure 2.** The result of physical characterization: a. FTIR spectra of Polymers; b. images from a scanning electron microscope of polymers; c. The outcome of Particle size analysis (PSA);d. The outcome of BET (Brunauer, Emmett, and Teller).

method are called MIP2 and NIP2.

3.5. Physical characterization

FTIR analysis identified the functional groups in the synthesized polymer and confirmed the polymerization process’s success. Figure 2a shows the results of the FTIR analysis of NIP, MIP, and MIP before and after extraction. Based on their FTIR spectra, the functional groups of MIP and NIP sorbents are identical. The polymerization process was successful because there were no doublet peaks near wavenumber 900–1000 cm<sup>-1</sup>, which indicated the absence of a vinyl group (-CH=CH2).<sup>33</sup>

The surface characteristics of MIP and NIP polymers were measured using a scanning electron microscope to observe the features up close. The NIP’s surface was smoother and less porous than the MIPs’, which had a rough surface with many pores, as shown by the SEM micrograph (Figure 2b). The uneven, rough, and porous surface of the MIPs was probably caused by the removal of the template, which also created the precise positions of the rebinding cavities, the structural properties of the MIPs point to a higher adsorption capacity.<sup>34</sup>

PSA was utilized to generate data on particle size distribution. MIP particle laser diffraction analysis can

be used to determine the volume size distribution. The physical characteristics of small, evenly sized nanoparticles are required for MIP synthesis to create a more stable protective barrier.<sup>35</sup> Figure 2c showed that the MIP2 particles were significantly smaller than the MIP1 particle

The BET technique assumes the uniformity of the pore walls. During MIP polymerization, the presence of template molecules affects the porosity and surface area of MIPs. We utilized the nitrogen adsorption data to compute the BET surface area. Figure 2d shows that MIP2 had a specific surface area of 2483.27 m<sup>2</sup>/g while MIP1 had a particular surface area of 2164.48 m<sup>2</sup>/g. Because of the gaps the imprinting process leaves behind, MIP has a is roughly three times more specific surface area than NIP.<sup>25</sup> The surface area of MIP is increased by the imprinting of template molecules, as demonstrated by SEM and BET characterization studies.

3.6. Evaluation of MIP and NIP adsorption capacity

Using adsorption isotherm models, we calculated the adsorption capacity of MIP and NIP. Table 3 displays the adsorption capacity values. Changes in polymer adsorption intensity show significant variations in binding site affinity. The Freundlich isotherm best characterized MIP2, suggesting the heterogeneous nature of the binding sites, while the Langmuir

**Table 3.** The outcome of adsorption capacity

Polymer	R <sup>2</sup>	Langmuir		R <sup>2</sup>	Freundlich	
		KL (L.mg)	Qm (mg.g <sup>-1</sup> )		m	KF (mg.g <sup>-1</sup> )
MIP 1	0.9994	0.9843	3.6532	0.9643	0.2327	0.8532
NIP 1	0.9653	0.4253	1.4367	0.9324	0.9642	0.1964
MIP 2	0.9842	0.7542	3.8426	0.9965	0.3763	1.8426
NIP 2	0.9853	0.4325	1.6532	0.9753	0.9532	0.3295

isotherm better characterized MIP1, indicating the homogenous nature of the binding sites, based on the correlation coefficients.<sup>36</sup> These findings suggest that, in contrast to MIP1, MP2 has a range of binding sites. Modifications in binding sites are linked with variations in polymer intensity. Binding site differences are correlated with variations in the degree of polymer adsorption capability.<sup>37</sup>

### 3.7. Removing OTC from spiked chicken meat with MIP

In the absorption capacity test, we used the optimum solvent for chloroform to improve the extraction conditions, using a standard solution of 2 mg/l TC. We examined the solvent SPE parameters for preconditioning, loading, washing, and elution. Chloroform was utilized to identify the solvent used in the conditioning step after examining vials containing MIP and NIP.

The polymer network will be impacted by modifications to the ' surface area and pore volume brought about by organic solvents. We filled it with chloroform, a solvent. To guarantee a successful MIP interaction, the loading solvent's polarity must be considered. Because of its low polarity and lack of prediction to obstruct the MIP–TC interaction, chloroform was our choice.<sup>38</sup>

After optimizing the adsorption parameters, we found that using chloroform as a solvent resulted in the highest TC adsorption %. The loading process was carried out six times during sonication, lasting 10, 15, 20, 25, 30, 40, and 50 minutes each time. Figure 3a shows the optimal loading time was 25 min for MIP2 and 50 min for MIP1. The washing optimization step needs to be completed next. Washing is, therefore, a crucial phase in the MIP-SPE process. Selecting

suitable solvents during the washing phase is a popular strategy to lessen nonspecific absorption difficulties. Achieving high extraction recoveries requires breaking strong trace–analytical interactions TC's protonation is anticipated to make it easier for the hydrogen bonds separating TC and MIPs to break.<sup>39</sup>

Elution was assessed using six loading contacts and one milliliter of elution liquid. Using 1 cc of elution solvent and six loading contact times of 10, 15, 20, 25, 30, 40, and 50 minutes we investigated elution to determine the best recovery. The optimal loading times for MIP1 and MIP2 were 50 and 25 minutes, respectively. After 50 minutes of loading, MIP1 had an ultimate recovery of  $84.78\% \pm 08.32\%$ , and NIP2 had an ultimate recovery of  $29.24\% \pm 8.01\%$  (Figure 3b). The ultimate recovery rates for MIP2 and NIP2 were  $95.16\% \pm 10.25\%$  and  $34.56 \pm 8.21$  percent, respectively, after a 25-minute loading time.

Using chicken meat treated with 2 mg/l TC in chloroform, we assessed the effectiveness of MI-SPE1 and MI-SPE2 in removing TC from the meat (using, NIP1 and NIP2). MI-SPE and NI-SPE were contrasted. We performed three experiments and computed the recovery and imprinting factor (IF) to assess each test's repeatability. A good imprint is shown by an IF > 1 that shows the distribution of a particular analyte in the MIPs compared to the NIPs.<sup>40</sup> With MI-SPE2, an average recovery of  $92.14 \pm 6.1\%$  was achieved, while NI-SPE 2 produced an average recovery percentage of  $34.63\% \pm 3.15\%$  with an IF of 2.66 (Figure 3c).

We evaluated MIPs' selectivity for removing TC from spiked chicken boiler meat compared to OTC and CTC, two additional medications that are derivatives of tetracycline antibiotics. Since OTC and CTC share a structure with TC, they were selected. We added 2 mg/l of each drug to the chicken boiler meet For TC,

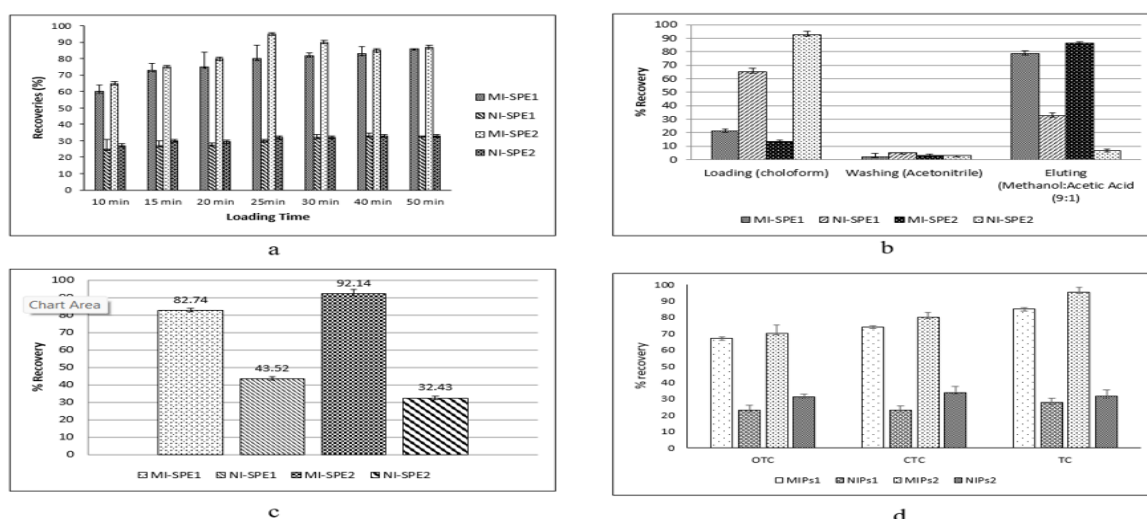


**Figure 3.** The result of the use of MIP to extract TC from spiked chicken boiler meat: a loading time's impact on recoveries; b. the MI-SPE and NI-SPE optimization; c. the recoveries of MI-SPE and NI-SPE on extraction TC from spiked chicken boiler meat; d. the selectivity test of MI-SPE and NI-SPE

the recovery percentage of MI-SPE1 was  $84.63 \pm 8.61\%$ ; for OTC it was  $66.9 \pm 6.48\%$ ; and for CTC it was  $73.91\% \pm 3.8\%$ . For TC, it was  $92.36 \pm 6.32\%$ ; for OTC it was  $70.23 \pm 4.25\%$ ; and for CTC, it was  $79.96 \pm 4.25\%$  in terms of MI-SPE2 recovery percentage (Figure 3d). Overall, MI-SPE demonstrated strong TC selectivity.

#### 4. Discussion

This study conducts a comprehensive examination of the formulation and utilization of Molecularly Imprinted Polymers (MIPs) aimed at the selective adsorption and elimination of tetracycline (TC), emphasizing improvements in adsorption efficiency, specificity, and practical implementation. By integrating computational modeling, empirical validation, and analytical characterization, this research establishes a solid foundation for the design of highly selective MIPs. The amalgamation of diverse experimental methodologies and practical assessments has led to an in-depth understanding of how functional monomers, polymerization techniques, and surface characteristics impact MIP performance.

The cornerstone of this investigation is the selection of methacrylic acid (MAA) as the most suitable functional monomer for TC imprinting. Computational modeling determined that MAA exhibits the most stable interaction with the TC template, featuring the lowest interaction energy ( $\Delta E = -29.40$  kcal/mol), thus surpassing other frequently employed monomers such as itaconic acid (ITA) and methyl methacrylate (MMA). This low  $\Delta E$  signifies a robust and stable complex between TC and MAA, essential for creating highly selective binding cavities within the polymer matrix.<sup>25</sup> The methanol-chloroform (1:1) solvent system was identified as the optimal medium for enhancing these interactions, resulting in the highest association constant ( $K_a = 2749.32$  M<sup>-1</sup>) for the TC-MAA complex. This solvent blend optimally balances the solubility of monomers and templates while facilitating ideal interactions during the polymerization phase, thereby fostering the development of selective binding sites.<sup>30</sup>

The structural characterization of molecularly imprinted polymers (MIPs) and their comparison with non-imprinted polymers (NIPs) offered critical insights into their superior adsorption capabilities. Scanning electron microscopy (SEM) analysis indicated that MIPs possess a rough and porous surface structure resulting from removing the template (TC), which leaves behind distinct cavities designed explicitly for the TC molecule.<sup>37</sup> In contrast, NIPs displayed smoother, less porous surfaces due to the absence of template-driven imprinting. BET surface area analysis corroborated the effects of the imprinting process, revealing that MIPs exhibited surface areas nearly

three times greater than those of NIPs (for example, MIP2 at  $2483.27$  m<sup>2</sup>/g compared to NIP2 at  $426.34$  m<sup>2</sup>/g). This augmented surface area, coupled with the specialized binding cavities, contributes to the enhanced adsorption performance of MIPs.<sup>40</sup>

Precipitation polymerization emerged as the preferred synthesis method, recognized for generating uniform, small particles with improved surface characteristics.<sup>20</sup> Compared to bulk polymerization, precipitation polymerization resulted in particles with more uniform size distribution and larger surface area, enhancing accessibility to the binding sites. Analysis of particle size indicated that precipitation-based MIPs had smaller dimensions (for instance, MIP2 measuring  $0.21$   $\mu$ m) in contrast to products from bulk polymerization, which leads to improved adsorption kinetics and increased adsorption capacity.<sup>31</sup> Moreover, this synthesis method demonstrated scalability, making it appropriate for practical applications. The adsorption performance of MIPs was further validated through batch adsorption studies and adsorption isotherm modeling. MIPs consistently outperformed NIPs in adsorption capacity across all tested solvents, with methanol-chloroform proving to be the optimal solvent for adsorption. Adsorption isotherm analysis revealed that MIP2 exhibited heterogeneous binding sites, as characterized by the Freundlich isotherm model, while MIP1 followed the Langmuir isotherm model, indicating homogeneity in binding site distribution.<sup>34</sup> The heterogeneous nature of MIP2's binding sites allows it to adapt to varying concentrations of TC, enhancing its adsorption efficiency under diverse conditions.<sup>36</sup>

Selectivity studies indicated that molecularly imprinted polymers (MIPs) exhibit greater specificity for tetracycline (TC) compared to structurally analogous tetracycline derivatives, such as oxytetracycline (OTC) and chlortetracycline (CTC). The precise molecular cavities generated during the imprinting process were customized to match the size, shape, and functional groups of TC, facilitating selective adsorption.<sup>34</sup> MI-SPE2 achieved a recovery rate of  $92.14 \pm 6.1\%$  for TC, significantly surpassing the OTC and CTC recovery rates, further validating the specificity inherent in the imprinting process. The imprinting factor (IF) of  $2.66$  for MI-SPE2 highlights the enhanced recognition and binding efficiency of MIPs relative to non-imprinted polymers (NIPs).

The practical application of MIPs in ensuring food safety was exemplified by their ability to eliminate TC from spiked chicken meat samples. The solid-phase extraction (SPE) procedure was optimized to maximize TC recovery. It utilizes chloroform as the preconditioning and loading solvent due to its low polarity and minimal interference with MIP-TC interactions.<sup>20</sup> The



washing and elution steps were meticulously refined to decrease nonspecific adsorption while maximizing recovery efficiency. After six adsorption cycles, MI-SPE2 consistently maintained a high recovery rate, demonstrating the reusability and cost-effectiveness of the MIPs. This stability and reusability position MIPs as an appealing option for large-scale food safety and environmental monitoring applications.<sup>17</sup>

Physical characterization further corroborated the reliability and robustness of the MIPs. Fourier-transform infrared (FTIR) spectroscopy validated successful polymerization and template removal while scanning electron microscopy (SEM) imaging and Brunauer-Emmett-Teller (BET) analysis underscored the structural advantages provided by the imprinting process. These comprehensive analyses offer compelling evidence that the MIPs developed in this study are structurally and functionally superior to their non-imprinted counterparts.<sup>29</sup>

## 5. Conclusions

Using the precipitation polymerization method, the MIP of TC with methacrylic acid as the functional monomer in a 1:1 methanol-chloroform combination performed well analytically, recovering  $92.36 \pm 6.32\%$ , for MI-SPE2 and  $34.63\% \pm 3.15\%$  for NI-SPE2. The sorbent's IF value is 2.66. According to the study, MIP TC is a suitable sorbent for extracting TC chicken boiler meat, which uses MAA as a monomer mixture of methanol and chloroform (1:1), manufactured by the precipitation polymerization method.

## Acknowledgment

We thanked the Republic of Indonesia's Ministry of Research and Higher Education for funding the study through the Fundamental Research Grant year 2024.

## Conflict of Interest

The authors declare no conflicts of interest.

## References

1. Arabsorkhi B, Sereshti H. Determination of tetracycline and cefotaxime residues in honey by micro-solid phase extraction based on electrospun nanofibers coupled with HPLC. *Microchem J* [Internet]. 2018;140(April):241–7. Available from: <https://doi.org/10.1016/j.microc.2018.04.030>
2. Han S, Jin Y, Su L. Analytical Methods crystal sensor for highly efficient tetracycline. 2020;
3. Spectrometry C, Furi M, Sinaga S, Lux E De. Analysis of Amoxicillin and Tetracycline Residues in Chicken Meat Using High Performance Liquid. 2018;01(2):14–20.
4. Rukmana P.M., Eksan S, Karmana S, R.Y L. Residual content of Tetracycline HCl in Poultry Product (Meat and Liver) as a Result of Giving Feed Additive For The Whole Life. *Media Vet*. 2011;5 (1):17–22.
5. Singh SP, Pundhir A, Ghosh S. Validation of an analytical methodology for determination of tetracyclines residues in honey by UPLC-MS/MS detection. *Indian J Nat Prod Resour*. 2015;6(4):293–8.
6. Cui J, Xie A, Liu Y, Xue C, Pan J. Fabrication of multi-functional imprinted composite membrane for selective tetracycline and oil-in-water emulsion separation. *Compos Commun* [Internet]. 2021;28(October):100985. Available from: <https://doi.org/10.1016/j.coco.2021.100985>
7. Nofita N, Rinawati R, Qudus HI. Validasi Metode Matrix Solid Phase Dispersion (MSPD) Spektrofotometri UV untuk Analisis Residu Tetrasiklin dalam Daging Ayam Pedaging. *J Kesehat*. 2016;7(1):136.
8. Putri MA, Herawati D, Nety K. Pengembangan metode analisis antibiotik tetrasiklin dalam hati ayam menggunakan kromatografi cair kinerja tinggi (KCKT). *Pros Penelit Sivitas Akad Unisba (Kesehatan dan Farm*. 2015;2:79–85.
9. Andini A. Analisis Residu Antibiotik Tetrasiklin Pada Daging Ayam Broiler Dan Daging Sapi. *J SainHealth*. 2019;3(2):33.
10. Aniza SN, Andini A, Lestari I. Analisis residu antibiotik tetrasiklin pada daging ayam broiler dan daging sapi. *J SainHealth*. 2019;3(2):22.
11. Baazize-Amami D, Dechicha AS, Tassit A, Gharbi I, Hezil N, Kebbal S, et al. Screening and quantification of antibiotic residues in broiler chicken meat and milk in the central region of Algeria. *Rev Sci Tech*. 2019;38(3):863–77.
12. Dhongade S, Pardeshi S, Kumar A. Molecularly Imprinted Microspheres for the Remediation of 2, 4-Dichlorophenol from Wastewater Using ' Template Analogue Imprinting Strategy .' 2017;11(2):17–23.
13. Zhao XF, Duan FF, Cui PP, Yang YZ, Liu XG, Hou XL. A molecularly imprinted polymer decorated on graphene oxide for the selective recognition of quercetin. *Xinxing Tan Cailiao/New Carbon Mater* [Internet]. 2018;33(6):529–43. Available from: [http://dx.doi.org/10.1016/S1872-5805\(18\)60355-5](http://dx.doi.org/10.1016/S1872-5805(18)60355-5)
14. Bakhtiar S, Bhawani SA, Shafqat SR. Synthesis and characterization of molecular imprinting polymer for the removal of 2 - phenylphenol from spiked blood serum and river water. *Chem Biol Technol Agric* [Internet]. 2019;1–10. Available from: <https://doi.org/10.1186/s40538-019-0152-5>
15. Krishnan H, Islam AKMS, Hamzah Z, Nadaraja P, Ahmad MN. A novel molecular imprint polymer synthesis for solid phase extraction of andrographolide. *Indones J Chem*. 2019;19(1):219–30.
16. Hasanah AN, Soni D, Pratiwi R, Rahayu D, Megantara S. Synthesis of Diazepam-Imprinted Polymers with Two Functional Monomers in Chloroform Using a Bulk Polymerization Method. 2020;2020.
17. Zamruddin NM, Herman H, Asman S, Hasanah AN. Synthesis and characterization of magnetic molecularly imprinted polymers for the rapid and selective determination of clofazimine in blood plasma samples. *Heliyon* [Internet]. 2024;10(13):e33396. Available from: <https://doi.org/10.1016/j.heliyon.2024.e33396>

18. Kartasasmita RE, Hasanah AN, Ibrahim S. Synthesis of selective molecularly imprinted polymer for solid-phase extraction of glipizide by using a pseudo-template. *J Chem Pharm Res.* 2013;5(10):351–5.
19. Hasanah AN, Rahayu D, Pratiwi R, Rostinawati T, Megantara S, Saputri FA, et al. Extraction of atenolol from spiked blood serum using a molecularly imprinted polymer sorbent obtained by precipitation polymerization. *Heliyon* [Internet]. 2019;5(4):e01533. Available from: <https://doi.org/10.1016/j.heliyon.2019.e01533>
20. Hasanah ANUR, Yulianti AB, Rahayu D. SELECTIVE ATENOLOL DETERMINATION IN BLOOD USING MOLECULAR IMPRINTED POLYMER WITH ITACONIC ACID AS FUNCTIONAL MONOMER. 2019;11(1).
21. Hasanah AN, Susanti I, Marcellino M, Maranata GJ, Saputri FA, Pratiwi R. Microsphere molecularly imprinted solid-phase extraction for diazepam analysis using itaconic acid as a monomer in propanol. *Open Chem.* 2021;19(1):604–13.
22. Nicholls IA, Karlsson BCG, Olsson GD, Rosengren AM. Computational strategies for the design and study of molecularly imprinted materials. In: *Industrial and Engineering Chemistry Research.* 2013. p. 13900–9.
23. Hammam MA, Abdel-Halim M, Madbouly A, Wagdy HA, El Nashar RM. Computational design of molecularly imprinted polymer for solid phase extraction of moxifloxacin hydrochloride from Avalox® tablets and spiked human urine samples. *Microchem J* [Internet]. 2019;148:51–6. Available from: <https://doi.org/10.1016/j.microc.2019.04.063>
24. Ahmadi F, Karamian E. Computational aided-molecular imprinted polymer design for solid phase extraction of metaproterenol from plasma and determination by voltammetry using modified carbon nanotube electrode. *Iran J Pharm Res.* 2014;13(2):417–30.
25. Suryana S, Mutakin M, Rosandi Y, Hasanah AN. Rational design of salmeterol xinafoate imprinted polymer through computational method: Functional monomer and crosslinker selection. *Polym Adv Technol.* 2022;33(1):221–34.
26. Suryana S, Mutakin M, Rosandi Y, Hasanah AN. Molecular Dynamic Study of Mechanism Underlying Nature of Molecular Recognition and the Role of Crosslinker in the Synthesis of Salmeterol-Targeting Molecularly Imprinted Polymer for Analysis of Salmeterol Xinafoate in Biological Fluid. *Molecules.* 2022;27(11).
27. Pratiwi R, Megantara S, Rahayu D, Pitaloka I, Hasanah AN. Comparison of Bulk and Precipitation Polymerization Method of Synthesis Molecular Imprinted Solid Phase Extraction for Atenolol using Methacrylic Acid. *J Young Pharm.* 2018;11(1):12–6.
28. Hasanah AN, Dwi Utari TN, Pratiwi R. Synthesis of Atenolol-Imprinted Polymers with Methyl Methacrylate as Functional Monomer in Propanol Using Bulk and Precipitation Polymerization Method. *J Anal Methods Chem.* 2019;2019.
29. Ahmad AL, Lah NFC, Low SC. Configuration of molecular imprinted polymer for electrochemical atrazine detection. *J Polym Res.* 2018;25(11).
30. Yang J, Li Y, Wang J, Sun X, Cao R, Sun H, et al. Molecularly imprinted polymer microspheres prepared by Pickering emulsion polymerization for selective solid-phase extraction of eight bisphenols from human urine samples. *Anal Chim Acta.* 2015 May;872:35–45.
31. Hasanah AN, Rahayu D, Pratiwi R, Rostinawati T. Extraction of atenolol from spiked blood serum using a molecularly imprinted polymer sorbent obtained by precipitation polymerization. *Heliyon* [Internet]. 2019;(December 2018):e01533. Available from: <https://doi.org/10.1016/j.heliyon.2019.e01533>
32. Cai W, Gupta RB. Molecularly-imprinted polymers selective for tetracycline binding. *Sep Purif Technol.* 2004;35(3):215–21.
33. Hasanah AN, Suryana S, Mutakin, Rahayu D. Evaluation performance of molecularly imprinted polymer prepared by two different polymerization method for atenolol recognition in human plasma. *Asian J Chem.* 2017;29(11):2429–33.
34. Hasanah AN, Yulianti AB, Rahayu D. Selective atenolol determination in blood using molecular imprinted polymer with itaconic acid as functional monomer. *Int J Appl Pharm.* 2019;11(1):136–43.
35. Susanti I, Triadenda AL, Murdaya N, Rahayu D, Pratiwi R, Rosandi Y, et al. Synthesis of multi-template molecularly imprinted polymers ( MT-MIPs ) for isolating ethyl para-methoxycinnamate and ethyl cinnamate from *Kaempferia galanga* L ., extract with methacrylic acid as functional monomer. 2024;
36. Ahmadi F, Ahmadi J, Rahimi-Nasrabadi M. Computational approaches to design a molecular imprinted polymer for high selective extraction of 3,4-methylenedioxymethamphetamine from plasma. *J Chromatogr A* [Internet]. 2011;1218(43):7739–47. Available from: <http://dx.doi.org/10.1016/j.chroma.2011.08.020>
37. Zhang K, Zou W, Zhao H, Dramou P, Pham-Huy C, He J, et al. Adsorption behavior of a computer-aid designed magnetic molecularly imprinted polymer via response surface methodology. *RSC Adv* [Internet]. 2015;5(75):61161–9. Available from: <http://dx.doi.org/10.1039/C5RA10367C>
38. Li H, Chen J, Tan L, Wang J. Solid-phase extraction using a molecularly imprinted polymer for the selective purification and preconcentration of norfloxacin from seawater. *Anal Lett* [Internet]. 2019;52(18):2896–913. Available from: <https://doi.org/10.1080/00032719.2019.1628245>
39. Wang L, Fu W, Shen Y, Tan H, Xu H, McPhee DJ. Molecularly imprinted polymers for selective extraction of Oblongifolin C from *garcinia Yunnanensis* Hu. *Molecules.* 2017;22(4):1–14.
40. Li J, Zhang L, Fu C. The Recognizing Mechanism and Selectivity of the Molecularly Imprinting Membrane [Internet]. *Molecularly Imprinted Catalysts: Principles, Syntheses, and Applications.* Elsevier Inc.; 2016. 159–182 p. Available from: <http://dx.doi.org/10.1016/B978-0-12-801301-4.00008-6>